High-throughput diffusion multiples

by J.-C. Zhao[†]*, Xuan Zheng[‡], and David G. Cahill[‡]

A diffusion multiple is an assembly of three or more different metal blocks, in intimate interfacial contact, subjected to high temperature to allow thermal interdiffusion to create solid-solution compositions and intermetallic compounds. Using microscale probes, composition-structure-phase-property relationships can be established with an efficiency orders of magnitude higher than conventional one-composition-at-a-time practice. For structural materials, such relationships include phase diagrams, diffusion coefficients, precipitation kinetics, solution strengthening effects, and precipitation strengthening effects. Many microscale probes can also be used to study several materials phenomena. For instance, microscale thermal conductivity measurements can be used to study order-disordering transformation, site preference in intermetallic compounds, solid-solution effect on conductivity, and compositional point defect propensity. This article will use a few examples to illustrate the capabilities and developmental needs of this approach.

[†]General Electric Company, GE Global Research,
1 Research Circle, Niskayuna, New York 12309, USA
*E-mail: zhaojc@research.ge.com

[‡]Department of Materials Science and Engineering,
University of Illinois at Urbana-Champaign,
Urbana, IL 61801, USA

The diffusion-multiple approach – the creation of composition gradients and intermetallic phases by long-term annealing of junctions of three or more phases/alloys – enables the study of phase diagrams, kinetics, and composition-structure-property relationships of bulk alloys[1-6]. It grew out of traditional diffusion couples and diffusion triples[7,8], which have been used to determine diffusion coefficients and phase diagrams for several decades. In addition to mapping phase diagrams based on the local equilibrium at the phase interfaces, Zhao[1,2] took advantage of the fact that the thermal interdiffusion process in diffusion couples and triples can generate complete single-phase compositions of solid solutions and intermetallic compounds in binary and ternary systems. By performing localized microscale property measurements on single-phase compositions, many composition-structure-property relationships can be mapped. The term 'diffusion multiple' was coined to reflect its development from diffusion couples/triples: (i) a new sample-making process using hot isostatic pressing (HIP) allows multiple diffusion couples and triples to be included in a single sample, creating a diffusion multiple; and (ii) localized property measurements allow many properties to be mapped in addition to phase diagrams, significantly extending applications of the methodology in materials research and discovery.

ISSN:1369 7021

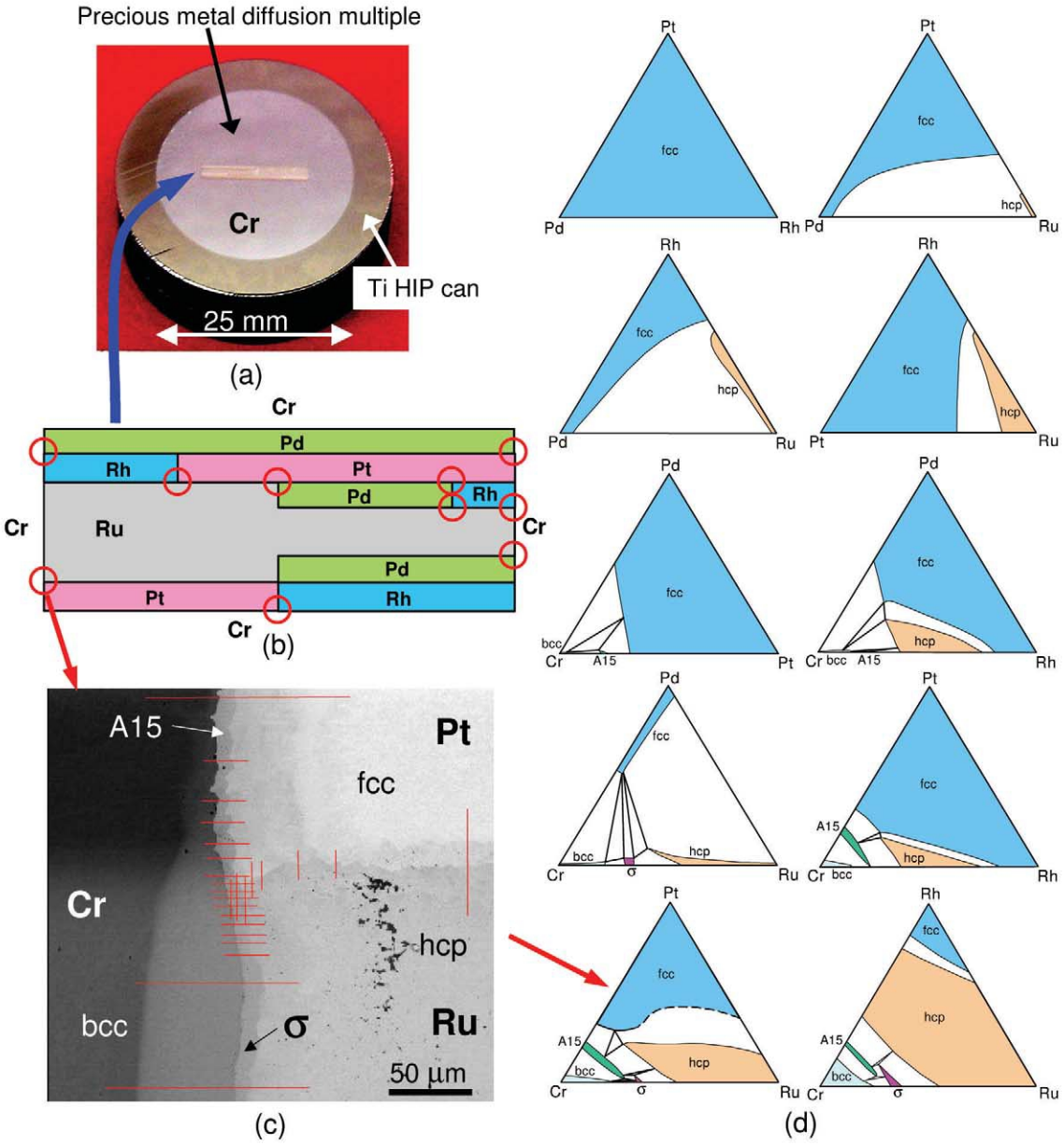

Fig. 1 Diffusion multiple for rapid mapping of ternary phase diagrams in the Pd-Pt-Rh-Ru-Cr system[5,9]. (a) Optical image of sample. (b) Arrangement of precious-metal foils to create many trijunctions (circles). (c) Backscattered electron image of Cr-Pt-Ru trijunction, showing formation of A15 ($Cr_3(Pt,Ru)$) and σ ($Cr_y(Ru,Pt)_x$) phases resulting from interdiffusion of Pt, Ru, and Cr, as well as electron microprobe scan locations. (d) Ten ternary phase diagrams (isothermal sections at 1200°C) obtained from this single diffusion multiple. Phase diagrams are plotted on atomic percent axes, with the scales removed for simplicity. (Reprinted with permission from[5]. © 2004 Springer.)

As an example, a diffusion multiple of Cr-Pd-Pt-Rh-Ru is shown in Fig. 1[5,9]. It was made by cutting a slot 1.8 mm in width and 12.7 mm in length in a disk of pure Cr 25 mm in diameter. Pure Pd, Pt, and Rh foils 0.25 mm thick, along with a piece of pure Ru, were arranged in a bricklaying geometry (Fig. 1b) and placed in the slot in the Cr disk. The brick pattern allows the formation of ten diffusion triples (trijunctions), shown in Fig. 1b by circles, in addition to many diffusion couples. When annealed, each triple creates a complete library of the single-phase compositions of that ternary system (see below). Intimate interfacial contact was achieved using a HIP process. (Details of the sample-making process can be found elsewehere[5,9].) The diffusion multiple was annealed at 1200°C for 40 hours. The diffusion time was chosen to develop diffusion profiles measurable over lengths of ~100 μm, so that neighboring diffusion sources would not interfere with the diffusion couples and triples being evaluated. The diffusion multiple was then cut, ground, and

polished for electroprobe microanalysis (EPMA), electron backscatter diffraction (EBSD), nanoindentation, and thermal conductivity evaluation.

A scanning electron microscopy (SEM) backscattered electron (BSE) image of the Cr-Pt-Ru trijunction is shown in Fig. 1c. The uppermost region, far from Ru, is essentially a binary diffusion couple of Cr-Pt. Based on the known binary phase diagram[10], there should be one intermetallic compound (Cr_3Pt with an A15 crystal structure) formed between Cr and Pt, in addition to the bcc and fcc solid solutions at 1200°C. There are no two-phase mixtures that are not allowed in binary diffusion couples. The lower region, far from Pt, is essentially a binary diffusion couple of Cr and Ru. One compound (σ, with a tetragonal crystal structure) has formed, consistent with the known binary Cr-Ru phase diagram[10]. The right-hand side, far from Cr, is essentially a binary diffusion couple of Pt-Ru, where no compound exists for this binary system, just the fcc and hcp solid solutions. Toward the center, where the three elements interdiffuse, ternary compositions are created by thermal diffusion, allowing measurement of the ternary phase diagram. It is difficult to locate the phase boundary between the A15 and the σ phase using the SEM BSE image alone; the EBSD technique is very useful in helping to identify the phases and their boundaries.

As is most often the case, no regions of two- or three-phase mixtures are formed during high-temperature diffusion heat treatment, although they may develop by precipitation reaction during cooling to ambient temperature. Two phases reach equilibrium at an interface and three phases equilibrate at a trijunction. The existence of local equilibrium at the phase interface was established many decades ago, and is the basis for applying diffusion couples to phase diagram determination[11,12]. The local equilibrium at phase interfaces and three-phase trijunctions in diffusion multiples is no different from that in diffusion couples, and is the basis for applying diffusion multiples to phase diagram determination.

EPMA scans were performed along the line locations shown in Fig. 1c. By taking advantage of the local equilibrium at the phase interfaces, the tie-line compositions were evaluated by extrapolating the concentration profiles to the phase interfaces. Based on the tie-line compositions obtained from all the EPMA scans shown in Fig. 1c, the entire isothermal section of the Cr-Rh-Ru ternary system was obtained (Fig. 1d). By performing similar analyses on all the ternary junctions (circled in Fig. 1b), a total of ten ternary phase diagrams were mapped from this single diffusion-multiple sample – it would probably take several hundred alloys to map these diagrams using conventional equilibrated alloy techniques. Thus, compared to the individual alloy method, there is an orders-of-magnitude increase in efficiency.

The applicability of the diffusion-multiple approach to the determination of very complex phase diagrams has been demonstrated for many systems[2,4,5,9]. A comparison of the phase diagrams determined using diffusion multiples and those determined using equilibrated alloys has been made for both simple and very complex ternary systems[5]. The results show clearly that the phase diagrams determined from diffusion multiples are very reliable.

In addition to phase diagram mapping, the most important feature of diffusion multiples is the ability to create complete single-phase composition ranges of solid solutions and intermetallic compounds of binary and ternary systems through interdiffusion process/reactions[1-6]. In this sense, a diffusion multiple serves as an efficient way of synthesizing many compositions and compounds in parallel in a single bulk sample, allowing many properties to be mapped as a function of composition, crystal structure, and phase. The enabling technologies for such property mapping are microscale property probes. Two of these – nanoindentation and thermal conductivity measurements – will be discussed as examples.

Mapping of Young's modulus

The localized measurement/mapping of Young's modulus using instrumented nanoindentation[13-16] is very straightforward. The load and displacement are monitored simultaneously during nanoindentation experiments. In simple terms, the initial slope of the unloading curve gives the elastic modulus (during initial unloading, the elastic deformation tries to push the indenter out). State-of-the-art corrections have been built into commercial nanoindenters to take into account friction, indenter and mechanical system compliance, and exact contact area calculation, etc. When care is exercised, measurement accuracy can be very high. A comparison between Young's modulus data measured from nanoindentation and those from handbook values show good agreement[17]. A force/load oscillation can be superimposed during loading, such that the elastic modulus can be evaluated from the loading curves, in addition to that from the initial unloading slope.

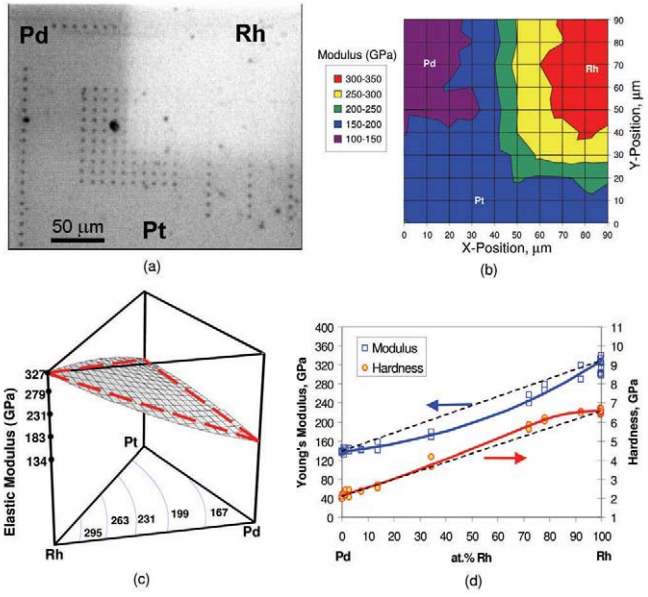

Fig. 2 Efficient mapping of Young's modulus versus composition using nanoindendation[3,9]. (a) Optical image of nanoindentation grid at the Pd-Pt-Rh trijunction region of the diffusion multiple in Fig. 1a. (b) Young's modulus contour plot obtained from (a). (c) Young's modulus data for Pd-Pt-Rh ternary system. (d) Hardness and Young's modulus variation with composition for Pd-Rh binary system, showing negative deviation from linear behavior for the modulus and slight positive deviation for hardness (solution hardening). (Parts (a), (c), and (d) reprinted with permission from[9]. © 2002 The Minerals, Metals & Materials Society.)

Young's modulus mapping of the Pd-Pt-Rh ternary system of the Cr-Pd-Pt-Rh-Ru diffusion multiple is shown in Fig. 2[3,9]. The Pd-Pt-Rh system is ideal for testing the capability of the technique, since Pd and Pt have very similar moduli. So, it constitutes a good test case to see if the technique is sensitive enough to differentiate between them. The Pd-Rh and Pt-Rh binary systems have very different moduli, so they provide a good test for seeing the trends; *ab initio* calculations predict different trends in elastic modulus for these two binary systems[18]. In addition, Pd, Pt, and Rh are completely soluble in one another at high temperature, so the ternary system provides a chance to map both the hardness and the modulus across the entire ternary solid solution field.

Nanoindentation scans were made for the entire Pd-Pt-Rh ternary system. An optical image taken after scans at the Pd-Pt-Rh trijunction is shown in Fig. 2a. EPMA analysis was performed after nanoindentation, in order to correlate the composition to the locations of the indents. The elastic moduli of the entire Pd-Rh-Pt ternary system are shown in Figs. 2b and 2c. The contour lines representing modulus levels are interpolated from the individual measurements.
A negative deviation from a linear rule-of-mixtures modulus (dashed line) can be seen for the Pd-Rh binary (Fig. 2d). For Pt-Rh, the modulus deviates slightly positively from linearity; for Pd-Pt, the modulus essentially follows the linearity for Pd-rich compositions, but deviates positively for Pt-rich compositions. Thus, the three-dimensional surface representing the compositional dependence of the modulus in the Pd-Rh-Pt system shows more complex behavior than a simple linear rule-of-mixtures. This complex behavior has been determined efficiently, both for alloying of elements with very different moduli (i.e. adding Rh to Pd-Pt mixes) as well as for alloying of elements with very similar moduli (i.e. adding Pt to Pd-Rh mixes of near-constant Rh content). It is interesting to note that the results are consistent with first-principles calculations of modulus for the binaries: negative deviation for Pd-Rh and positive deviations for both Pd-Pt and Pt-Rh[18]. The usefulness of the diffusion-multiple approach to efficiently generate the data needed to verify first-principles models should have an impact on the validation of fundamental models of alloying.

The current temperature capability of the instrumented nanoindentation apparatus is about -10°C to 200°C. Young's modulus can be measured readily over this temperature range. Poisson's ratio is required as an input during analysis. There has been effort to evaluate Poisson's ratio using a spherical indenter together with neural network analysis[19,20]. There are also other techniques for microscale modulus measurements – reviews of these techniques can be found elsewhere[21,22].

The solid-solution hardening effect can also be mapped in the same way as the Young's modulus[1-3,6,9].

Mapping of thermal conductivity

Thermal conductivity is an important property for applications ranging from gas turbine blades through microelectronic devices to thermoelectric units. For metals and intermetallic compounds, heat conduction is carried predominantly by free electrons. Therefore, the thermal conductivity of these materials is very sensitive to elemental substitution, point defect formation, and ordering, and can be used to study these phenomena. Elemental substitution and point defect formation decrease the thermal conductivity, since both increase electron scattering. Ordering in crystals decreases the electron scattering and thus increases thermal conductivity. Thermal conductivity is not very sensitive to microstructural features such as dislocations and

grain boundaries (unless the grain size approaches the nanometer scale). This is simply because the densities of dislocations and grain boundaries per unit volume are usually far less than those of point defects and elemental substitutions.

Thermal conductivity is generally correlated to electrical conductivity by the Wiedemann-Franz law for metals and intermetallic compounds[23,24], so it can be used to estimate the electrical conductivity. For insulating materials, thermal conductivity is carried by phonons and the Wiedemann-Franz law no longer holds. In this case, thermal conductivity measurement can be used to study lattice vibration.

An accurate, micronscale-resolution thermal conductivity mapping/measurement tool was recently developed using time-domain thermoreflectance with a femtosecond pulsed laser (Fig. 3a)[25,26]. A thin (e.g. 100 nm) Al film is first sputter coated on to a sample. This acts as a transducer to absorb the laser pulse and enables sensitive measurement of the temperature change via the relatively large thermoreflectance of Al at the wavelength of a Ti:sapphire laser (λ = 770 nm; because of a bandstructure feature, the optical reflectivity of Al at λ = 770 nm has a strong temperature dependence). The femtosecond-pulsed laser is split into two beams: the pump beam and the probe beam. The pump beam is modulated at ~10 MHz to limit lateral heat flow and heats the near-surface region of the Al film. As the heat diffuses through the sample, the surface temperature of the Al film decays, as does the Al reflectivity, which is monitored by the probe beam. The probe beam is modulated at audio frequencies to eliminate artifacts created by scattering of the pump beam by surface roughness. The thermal properties of the sample are evaluated by matching the temperature decay obtained from experiment with that calculated from heat flow models. The thermal effusivity (the square root of the product of the thermal conductivity Λ and heat capacity per unit volume C) is extracted from the ratio of in-phase to out-of-phase responses $V_{in}(t)/V_{out}(t)$ of the thermoreflectance at the modulation frequency of the pump beam.

The accuracy of the technique is benchmarked using some common metals and ceramic materials by measuring their thermal conductivities and comparing the results to well-accepted values. The results are plotted in Fig. 3b and show very good accuracy with a standard deviation of ±8%[26]. Note that Fig. 3b is not a calibration curve – the new technique yields thermal conductivity measurements directly without the use of such a curve. The thermal conductivity data are calculated directly from the change in thermoreflectance. Actually, the direct measurement is made for thermal effusivity but, since the heat capacities of common materials are known, the thermal conductivity data can be calculated readily. The measurement speed can easily reach 10 000 points per hour. The technique is applicable to essentially all materials (metals, ceramics, and polymers) as long as a thin film of Al can be sputtered onto the surface[24]. Also, this technique can be applied to map both bulk diffusion multiples (or metallographic mounts) and thin films (since the sensing depth of the technique is in the 200 nm range).

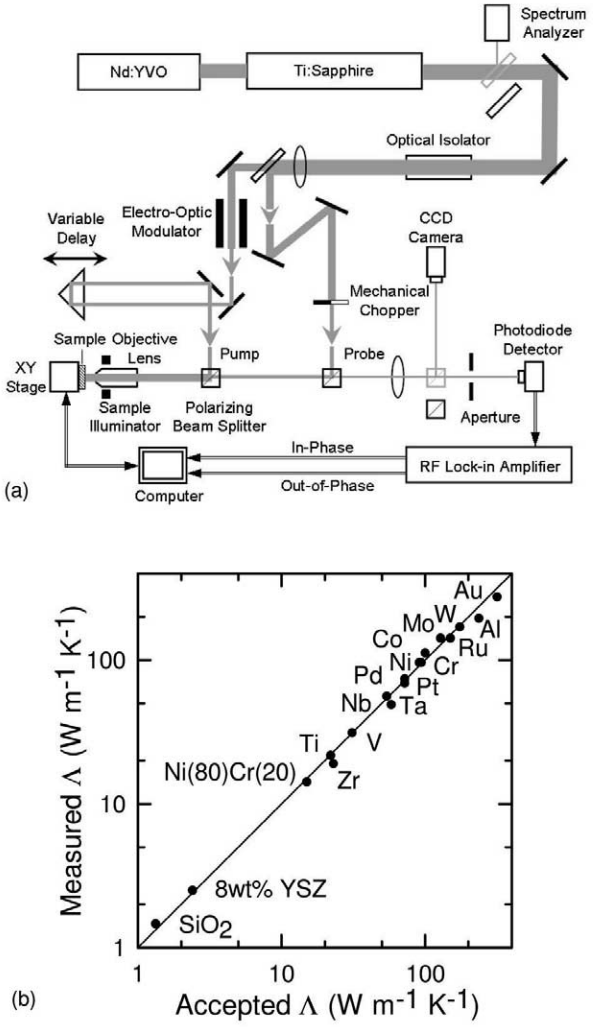

Fig. 3 An accurate, micronscale-resolution thermal conductivity measurement technique based on time-domain thermoreflectance[25-26]. (a) Measurement setup using femtosecond pulsed laser. (b) Comparison of measured thermal conductivity values with well-accepted handbook values of some common metals and ceramics to illustrate the accuracy.

Fig. 4 shows an application of thermal conductivity mapping in studying order-disorder transformations[26]. Fig. 4a is an SEM BSE image of the Cr-Pt binary diffusion couple (upper region of Fig. 1c) in the precious-metal diffusion multiple shown in Fig. 1. The thermal conductivity map of the same area is shown in Fig. 4b; the thermal conductivity values measured along the dashed line in Fig. 4b are shown in Fig. 4c. The increase in thermal conductivity above that of the disordered Pt-based fcc phase indicates the formation of ordered phases. On the basis of the Cr-Pt binary phase diagram shown in Fig. 4d[10,27,28], it can be deduced that the two peaks at ~100 μm and 125 μm correspond to formation of fcc superlattice structures $L1_0$ (CrPt) and $L1_2$ ($CrPt_3$), respectively. The Cr_3Pt phase did not show an increase in thermal conductivity above that of the disordered fcc phase, probably because Cr_3Pt has a completely different crystal structure, Cr_3Si-type (*cP4*). It is clear from Figs. 4b and 4c that a region of disordered fcc phase exists between the two ordered phases. The correct phase diagram feature related to the ordered phases is shown in Fig. 4d by dotted lines. This new version is more rational, since the CrPt and $CrPt_3$ phases have related, but different, crystal structures compared to the parent fcc phase. So, there should be two-phase regions around them (similar to the Cu-Au binary system). Note that the diffusion multiple was annealed at 1200°C, which is above the order-disorder transition temperatures of both the CrPt and $CrPt_3$ phases. Hence, the ordered phases were formed during cooling from 1200°C to room temperature. It can be seen that the ordering effect can be mapped very effectively using diffusion multiples and the novel mapping technique. Such mapping would otherwise be very time consuming and laborious using conventional techniques. Spatial mapping of ordering effects at micronscale resolution would otherwise require micro X-ray diffraction using a micronscale synchrotron beam.

Measurement/mapping of the solid solution effect on thermal conductivity can readily be done using the micronscale thermal conductivity mapping tool and diffusion multiples[22,26]. Thermal conductivity measurements can also be used to study compositional point defect formation. Point defects such as vacancies and antisites (where one element sits on the lattice site of the other element) have a crucial effect on the properties of intermetallic compounds and ceramic materials. For instance, the formation of point defects in NiAl results in a change of approximately three orders of

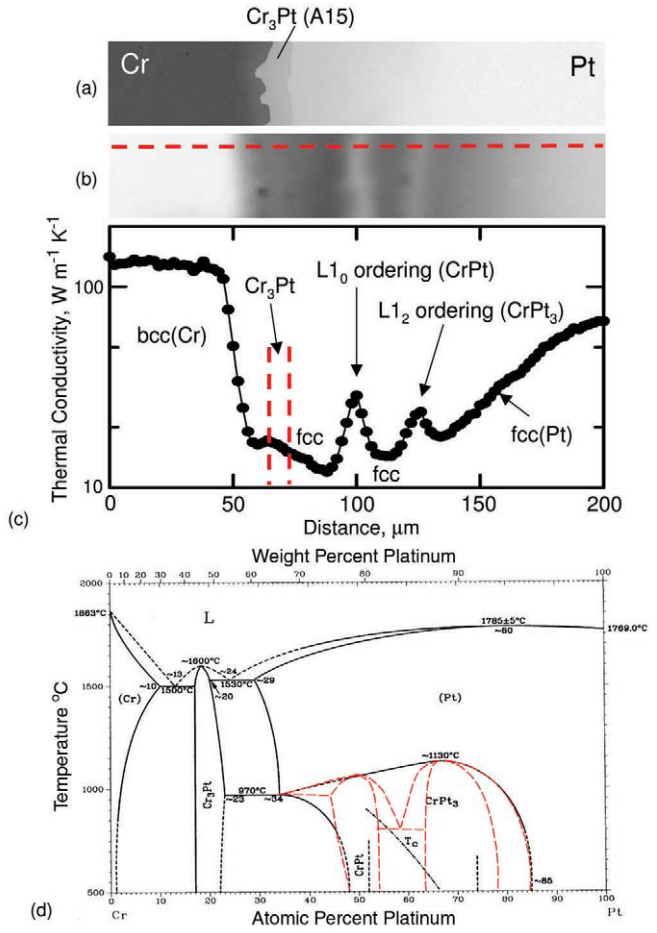

Fig. 4 Application of microscale thermal conductivity mapping to the study of ordering[26]. (a) SEM BSE image of upper region of Fig. 1c, showing the Cr-Pt binary diffusion couple (the image is 200 μm in width). (b) Thermal conductivity map of the same location. (c) Thermal conductivity values along the dashed line in (b) showing the increased thermal conductivity in regions where ordering occurs. (d) Proposed refinement (dotted lines) of the phase diagram showing the two ordered phases in separate phase regions and the disordered region between them.

magnitude in diffusion coefficients (Fig. 5c)[29]. The study of point defects is not a trivial process and usually involves careful measurements of density and lattice parameters in addition to structural characterization (making fully dense intermetallic compounds is often a challenge by itself). When the point defect population is high, it may be found through thermal (or electrical) conductivity measurements. An example is shown in Fig. 5 for NiAl. The thermal conductivity of NiAl varies sharply with composition (Fig. 5b)[30], which can be correlated to point defect formation in nonstoichiometric compositions. This has been well characterized using density and X-ray diffraction data (Fig. 5a)[31]. There is a high concentration of Ni vacancies in Al-rich compositions, varying from 0% at 50 at.% Al to 13% at 54 at.% Al (the results were based on samples water quenched from 1000°C).

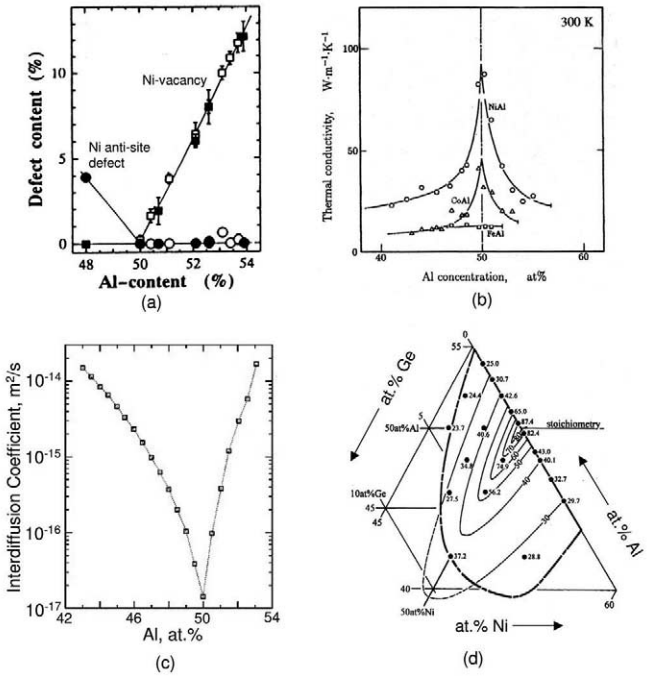

Fig. 5 Point defect formation and site preference in NiAl[26]. (a) Point defect type and concentration variations with composition in NiAl. (Reprinted with permission from[31]. © 1996 Elsevier.) (b) Thermal conductivity variation with composition for NiAl, CoAl, and FeAl[30]. (Reprinted with permission from[44]. © 1995 Elsevier.) (c) Variation in interdiffusion coefficients with composition for NiAl at 1000°C[29]. (d) Contour map of thermal conductivity in NiAl phase region of the Ni-Al-Ge system. The ridge direction indicates that Ge is substituting for Al in the NiAl phase[44-47]. (Reprinted with permission from[45]. © 2001 Springer.)

Similarly, the Ni antisite defects form in Al-lean compositions of NiAl, with concentration varying from 0% at 50 at.% Al to 4% at 48 at.%Al[31]. Such high point defect concentrations in nonstoichiometric NiAl are likely responsible for the thermal conductivity behavior shown in Fig. 5b. Similarly, the thermal conductivity of CoAl varies appreciably with concentration (Fig. 5b), which is also consistent with the varying amounts of point defects in nonstoichiometric compositions[32]. In contrast, the thermal conductivity of FeAl changes little with composition, even though there are appreciable amounts of point defects in FeAl varying with composition[33]. This is probably because the point defect (thermal vacancy) population, even at the stoichiometric composition of FeAl, is so high (which drives its conductivity to such a low value) that further increases in compositional point defects no longer make a difference to thermal conductivity. This interpretation is a subject for further study in the future. In any case, a strong composition dependence of thermal conductivity is sufficient, but not required, evidence for compositional point defect formation. In other words, when a large variation in thermal conductivity is observed over a very narrow composition range of an intermetallic compound, it is very likely that there is a high concentration of point defects, whereas the opposite is not always true.

Thermal conductivity measurements can also be used to study the site preference/elemental substitution in intermetallic compounds. As a third element is added into a binary intermetallic compound, it often preferentially substitutes for one element. Such information on elemental substitution (site preference) is critical for designing the strength of intermetallics[34,35] and is also essential for selecting the right sublattice models for thermodynamic CALPHAD (CALculation of PHAse Diagrams) modeling of the phase. For either a stoichiometric compound or a compound with a limited single-phase region, this information can be read directly from the direction of the binary phase into the corresponding ternary phase diagram, i.e. the direction of the so-called solubility lobe. For a nonstoichiometric compound with a wide single-phase region such as NiAl, such information cannot be deduced from the phase diagram. For instance, it is not possible to find from the Ni-Al-Ge ternary phase diagram whether Ge substitutes for Ni or Al or both. For such cases, there are many different ways to study elemental substitution[36-43]. However, these techniques often require stringent sample preparation or even single-crystal samples, which are not easy to prepare for brittle intermetallics. An alternative method is to extract the site preference information from the thermal conductivity contour map, as shown in Fig. 5d for the example of Ge in NiAl[44-47]. In the direction of elemental substitution, the thermal conductivity displays a ridge in the contour map, since the atom mixing in this direction is less random than other directions. Thus, it can be seen clearly that Ge preferentially substitutes for Al in NiAl. Again, a combination of diffusion multiples (to form complete single-phase compositions of intermetallic compounds) and the new measurement technique (to map thermal conductivity variation with composition) can be used to evaluate effectively the site preference/elemental substitution in intermetallic compounds.

Even though the thermal conductivity mapping tool has been developed for combinatorial/high-throughput measurements of combinatorial samples, it can also be used effectively for studying regular metallographic samples. An example is shown in Fig. 6 for a cross-sectional, regular

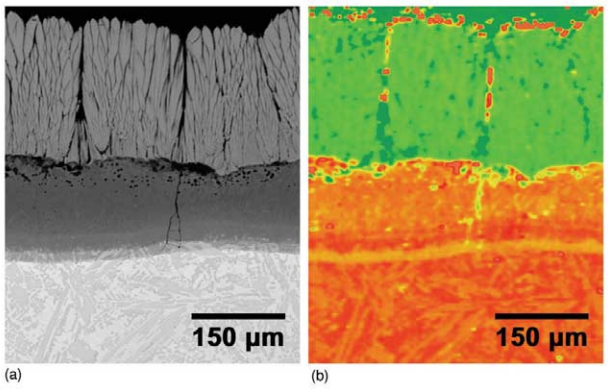

Fig. 6 Application of the microscale thermal conductivity mapping tool to study a regular metallographic sample[26]. (a) BSE image of a cross-sectional metallographic sample showing a yttria-stabilized zirconia (YSZ) thermal barrier coating (TBC) on the top, a multiphase bond coat in the middle, and a predominantly two-phase Nb silicide composite substrate at the bottom. (b) Thermal conductivity map of the same sample, showing the thermal conductivity of various materials and phases in the sample.

metallographic sample that contains a thermal barrier coating (TBC), a bond coat, and a substrate[26]. The thermal conductivity map reveals the different phases and provides the thermal conductivity values of each phase. In this regard, thermal conductivity of intermetallic compounds can be obtained without making single-phase samples.

Application to accelerate materials design and discovery

Application of the diffusion-multiple approach to designing alloys and performing effective materials research is summarized schematically in Fig. 7[6]. The left-hand side shows the application of diffusion multiples to map phase diagrams as an essential input into CALPHAD modeling to construct thermodynamic databases for the prediction of phase equilibria in multicomponent alloys. The diffusion-multiple approach can increase the efficiency of phase diagram mapping by orders of magnitude, making it possible to have phase diagrams available in advance of alloy design if the diffusion multiples are made early. This is particularly useful in developing completely new alloys. For the development of existing alloy systems, such as superalloys, the diffusion-multiple approach can be applied to obtain critical data to improve the predictability of the thermodynamic database.

Many binary diffusion profiles can be obtained from diffusion multiples to allow extraction of chemical diffusion coefficients. Because of the large number of profiles that are available, automated diffusivity extraction is imperative. It is

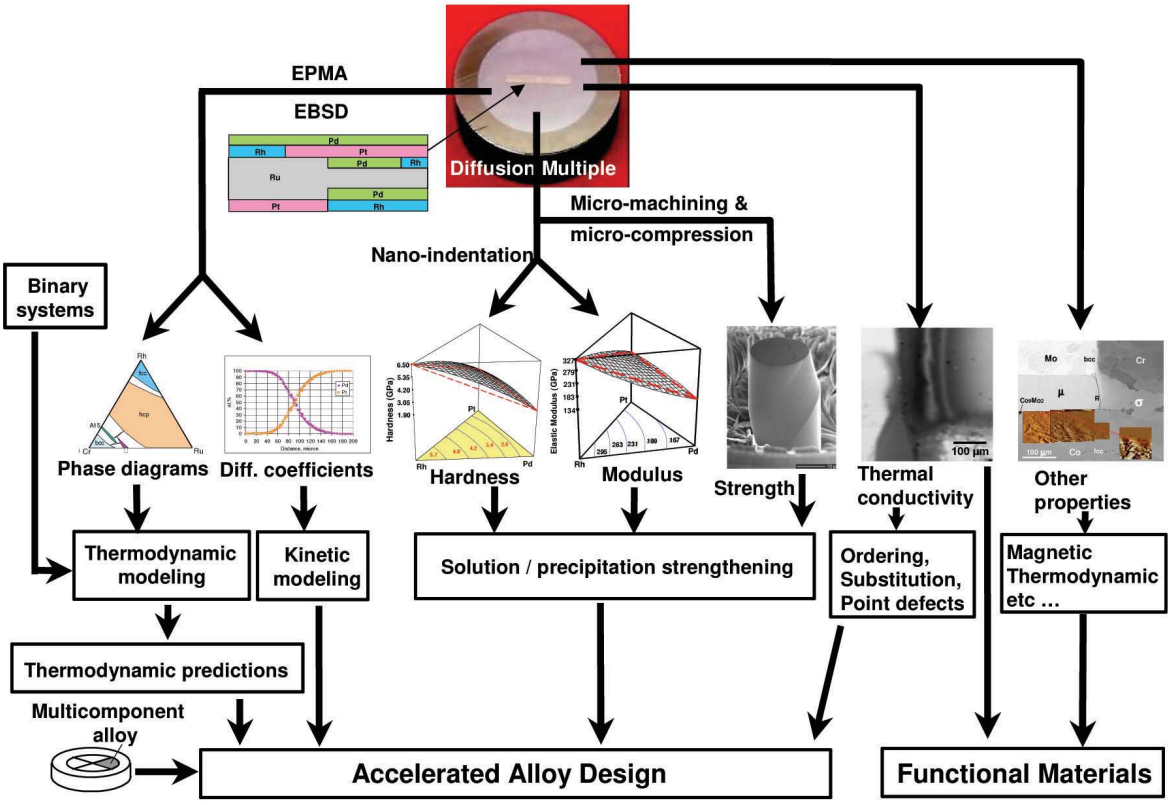

Fig. 7 Graphic summary of the diffusion-multiple approach to high-throughput materials research and discovery[3,6]. (Reprinted with permission from[6]. © 2005 Annual Reviews.)

important to develop robust algorithms to perform diffusivity data extraction from binary, multiphase diffusion profiles. The diffusivity database is essential for modeling nucleation kinetics, precipitation kinetics, and grain growth.

Also, diffusion multiples made of multicomponent alloys can be used to generate new compositions by interdiffusion. This allows direct screening of compressive strength using microcompression tests on micropedestals machined with focused ion beam (FIB), micro-electro-discharge machining (microEDM), or femtosecond laser techniques[6,22,48-52].

The central part of Fig. 7 illustrates the importance of hardness and modulus mapping for structural materials design. The solution-hardening effect is directly correlated to solution strengthening, which involves complex interactions. Mappings of hardness and modulus will provide critical data for alloy design and for testing first-principles predictions. A solution-hardening database can be constructed to allow alloy developers to pick effective elements for strengthening alloys[3,6]. This is particularly useful for alloy design in new alloy systems when the elemental selection needs to be made. Precipitation kinetics and precipitation-hardening effects can also be established using diffusion multiples coupled with nanoindentation and microstructure analysis[6].

In addition to mapping thermal conductivity itself for the discovery of functional materials such as thermoelectrics, the microscale thermal conductivity probe can be used to study order-disordering transformation, site preference in intermetallic compounds, solid-solution effect on conductivity, and compositional point defect propensity, as shown in Figs. 4 and 5. Such information is useful in the design of intermetallic compounds for various applications, especially for high-temperature strength. Thermal conductivity measurement has rarely been used as a research tool to study alloy substitution and ordering, simply because thermal conductivity is not a property that is easy to measure accurately and effectively. One exception is the work by Terada and coworkers[44-47], who effectively used thermal conductivity measurement to study elemental substitution/site preference. The development of the microscale technique[25,26] may make thermal conductivity measurement a common tool for materials science research. As more microscale property tools are developed to enable fast measurements of certain properties as a function of composition and phases in diffusion multiples or other combinatorial libraries, new ways to do research will emerge to facilitate the development of more composition-structure-property relationships for faster materials design.

The right-hand side of Fig. 7 emphasizes the potential of employing diffusion multiples to discover functional materials. This will be enabled by the development of many microscale property probes to allow mapping of physical, thermal, optical, magnetic, and other properties.

Limitations and development needs

In diffusion multiples, the formation of solid solutions and intermetallic compounds is at the mercy of the thermal interdiffusion process. At temperatures below half of the melting (solidus) temperature, it may take a long time to promote sufficient interdiffusion to form intermetallic compounds and solid solutions owing to the very slow diffusion kinetics. In addition, there is a danger of missing phases (where an equilibrium phase fails to form because of kinetic barriers) or the formation of nonequilibrium phases at relatively low temperatures. So, it is highly recommended that diffusion multiples are annealed at greater than half the melting temperature (the solidus of the binary and ternary systems).

Until now, diffusion multiples have been applied only to metals and alloys. Effort is now underway to extend the approach to study ceramic systems such as oxides. Since ceramic diffusion couples have been made before, there is no reason to doubt the applicability of the diffusion-multiple approach to ceramic systems. The key is to anneal the samples at very high temperatures to achieve sufficient interdiffusion.

Diffusion multiples put a much higher demand on the spatial resolution of the microscale property probes compared to thin-film-based combinatorial samples, for which spatial resolutions of hundreds of microns are usually sufficient. To analyze diffusion multiples, the spatial resolution of the microscale property probes should be <10-20 μm, and ideally ~1-5 μm. Fortunately, many microscale property probes have resolutions that are compatible with this requirement.

The key advantage of diffusion multiples is the formation of all equilibrium intermetallic compounds and solid-solution phases, with a complete range of all single-phase compositions for binary and ternary systems. Hence, diffusion multiples can constitute a combinatorial synthesis tool for the parallel generation of *bulk* intermetallic compounds and solid solutions. In this sense, diffusion multiples complement

thin-film combinatorial samples, where certain thickness-induced phenomena may occur.

In this article, only phase diagram mapping and the mapping of two properties – Young's modulus and thermal conductivity – have been chosen as examples to illustrate the power of the diffusion-multiple approach for effective materials research. Further information can be found in two comprehensive reviews[6,22] on state-of-the-art diffusion-multiple methodology and the microscale property probes that enable the methodology. Microscale probes of several properties, such as elastic modulus, hardness, thermal conductivity, dielectric properties, optical properties, and crystal structure, are relatively well developed[22]. The probes for electrical conductivity, magnetic properties, and compressive yield strength need either further improvement or more benchmark studies. The probes yet to be developed that would have a significant impact on materials research include those for lattice parameter measurement at microscale resolutions, localized melting point measurement, ductility, thermal expansion coefficients, and thermodynamic properties. The impact of the development of microscale probes goes beyond combinatorial materials research, since most of them can be applied to regular (noncombinatorial) metallographic or thin-film samples too. Robust microscale probes for electrical conductivity and thermodynamic quantities such as specific heat and heat of formation are among the most critical to be developed. Broader applications of the diffusion-multiple approach depend on development of these probes. MT

Acknowledgments

The authors are grateful to S. Balsone, R. W. Cahn, C. E. Campbell, E. L. Hall, M. F. Henry, S. Huxtable, M. R. Jackson, I. Matthew, L. A. Peluso, A. M. Ritter, S. D. Sitzman, J. A. Sutliff, and J. H. Westbrook for help, support, and/or valuable discussions. Parts of the work were supported by General Electric (GE) Company internal funding, the US Air Force Office of Scientific Research (AFOSR) under grant no. F49620-99-C-0026, the Defense Advanced Research Projects Agency (DARPA) under the Accelerated Insertion of Materials (AIM) program and grant no. F33615-00-C-5215, the US Department of Energy grant no. DEFG02-01ER45938, and the National Science Foundation grant no. CTS-0319235.

REFERENCES

1. Zhao, J.-C., *Adv. Eng. Mater.* (2001) **3** (3), 143
2. Zhao, J.-C., *J. Mater. Res.* (2001) **16** (6), 1565
3. Zhao, J.-C., *et al., MRS Bull.* (2002) **27** (4), 324
4. Zhao, J.-C., *et al., Acta Mater.* (2003) **51** (20), 6395
5. Zhao, J.-C., *J. Mater. Sci.* (2004) **39** (12), 3913
6. Zhao, J.-C., *Annu. Rev. Mater. Res.* (2005) **35**, 51
7. Hasebe, M., and Nishizawa, T., *Application of Phase Diagrams in Metallurgy and Ceramics*, Carter, G. C., (ed.), NBS, Washington DC, (1978) **2**, 911
8. Jin, Z., *Scand. J. Metall.* (1981) **10**, 279
9. Zhao, J.-C., *et al., JOM* (2002) **54** (7), 42
10. Massalski, T. B., *Binary Alloy Phase Diagrams*, 2nd edn., ASM International, Materials Park, OH, (1990)
11. van Loo, F. J. J., *Prog. Solid State Chem.* (1990) **20** (1), 47
12. Kodentsov, A. A., *et al., J. Alloys Comp.* (2001) **320** (2), 207
13. Doerner, M. F., and Nix, W. D., *J. Mater. Res.* (1986) **1** (4), 601
14. Oliver, W. C., and Pharr, G. M., *J. Mater. Res.* (1992) **7** (6), 1564
15. Fischer-Cripps, A. C., *Nanoindentation*, Springer, New York, (2004)
16. Cheng, Y.-T., and Cheng, C.-M., *Mater. Sci. Eng. R* (2004) **44** (4-5), 91
17. Hay, J. L., *private communication*, (2005)
18. Turchi, P. E. A., *private communication*, (2002)
19. Huber, N., *et al., ASME J. Appl. Mech.* (2001) **68** (2), 218
20. Huber, N., and Tsakmakis, Ch., *ASME J. Appl. Mech.* (2001) **68** (2), 224
21. Warren, O. L., and Wyrobek, T. J., *Meas. Sci. Technol.* (2005) **16** (1), 100
22. Zhao, J.-C., *Prog. Mater. Sci.* (2006) to be published
23. Klemens, P. G., and Williams, R. K., *Int. Met. Rev.* (1986) **31** (5), 197
24. Kumar, G. S., *et al., J. Mater. Sci.* (1993) **28**, 4261
25. Huxtable, S., *et al., Nat. Mater.* (2004) **3** (5), 298
26. Zheng, X., *et al.*, to be published
27. Waterstrat, R. M., *Metall. Mater. Trans. A* (1973) **4**,1585
28. Baglin, J., *et al., J. Electrochem. Soc.* (1978) **125**, 1854
29. Kim, S., and Chang, Y. A., *Metall. Mater. Trans. A* (2000) **31A** (6),1519
30. Terada, Y., *et al., Intermetallics* (1995) **3** (5), 347
31. Kogachi, M., *et al., Scripta Mater.* (1996) **34** (2), 243
32. Kogachi, M., and Tanahashi, T., *Scripta Mater.* (1996) **35** (7), 849
33. Kogachi, M., and Haraguchi, T., *Scripta Mater.* (1998) **39** (2), 159
34. Cotton, J. D., *et al., Intermetallics* (1993) **1** (1), 3
35. Pike, L. M., *et al., Intermetallics* (1997) **5** (8), 601
36. Miller, M. K., and Horton, J. A., *Scripta Metall.* (1986) **20** (8), 1125
37. Almazouzi, A., *et al., Intermetallics* (1997) **5** (1), 37
38. Chiba, A., *et al., Acta Metall. Mater.* (1991) **39** (1), 13
39. Munroe, P. R., and Baker, I., *J. Mater. Res.* (1991) **6** (5), 943
40. Bohn, H. G., *et al., Mater. Res. Soc. Symp. Proc.* (1987) **81**, 127
41. Lin, H., *et al., Mater. Res. Soc. Symp. Proc.* (1987) **81**, 165
42. Masahashi, N., *et al., Acta Metall.* (1988) **36** (7), 1815
43. Lin, H., and Pope, D. P., *J. Mater. Res.* (1990) **5** (4),763
44. Terada, Y., *et al., Intermetallics* (1995) **3** (5), 347
45. Terada, Y., *et al., J. Mater. Res.* (2001) **16** (8), 2314
46. Terada Y., *et al., Mater. Sci. Eng. A* (2002) **329-331**, 468
47. Terada Y., *et al., Mater. Trans.* (2002) **43** (12), 3167
48. Uchic, M. D., *et al., Mater. Res. Soc. Symp. Proc.* (2003) **753**, BB1.4.1
49. Uchic, M. D., *et al., Science* (2004) **305**, 986
50. Uchic, M. D., *private communication*, (2004)
51. Feng, Q., and Pollock, T., *private communication*, (2004)
52. Feng, Q., *et al., Superalloys 2004*, TMS, Warrendale, PA, (2004), 687